Progress In Electromagnetics Research B, Vol. 33, 291–315, 2011

PERFORMANCE ANALYSIS OF ANTENNA ARRAY BEAMFORMERS WITH MUTUAL COUPLING EFFECTS

J.-H. Lee[1,*] and Y.-L. Chen[2]

[1]Department of Electrical Engineering, Graduate Institute of Communication Engineering, and Graduate Institute of Biomedical Electronics and Bioinformatics National Taiwan University, No. 1, Section 4, Roosevelt Road, Taipei 10617, Taiwan

[2]Graduate Institute of Communication Engineering, National Taiwan University, No. 1, Section 4, Roosevelt Road, Taipei 10617, Taiwan

Abstract—Antenna array beamformers suffer from performance deterioration in the presence of mutual coupling (MC) between array sensors. In this paper, we present a theoretical analysis in terms of the output signal-to-interference-plus-noise ratio (SINR) for the performance of antenna array beamformers under MC effects. Based on the model of a distortion matrix to encapsulate the MC effects, a closed-form expression for the SINR is derived that is shown to accurately predict the SINR obtained in simulations. This theoretical formula is valid for any distortion matrix estimated from collected measurement data. The SINR formulas provide insights into the influence of the MC effects on the performances of the linearly constrained minimum variance (LCMV) beamformer and the eigenspace-based (ESB) beamformer. It is shown that the ESB beamformer outperforms the LCMV beamformer under MC effects. Moreover, we derive the formulas for computing the eigenvalues of signal correlation matrix under MC effects. Simulation results are presented for confirming the validity of the theoretical results.

Received 28 May 2011, Accepted 29 July 2011, Scheduled 5 August 2011

* Corresponding author: Ju-Hong Lee (juhong@cc.ee.ntu.edu.tw).

1. INTRODUCTION

In the literature, there are two popular antenna array beamformers, namely the linearly constrained minimum variance (LCMV) beamformer [1] and eigenspace-based (ESB) beamformer [2]. The LCMV beamformer finds its optimal weight vector $\mathbf{w}_{LCMV}$ by minimizing the beamformer output power with a linear constraint to ensure unit power gain in the desired signal direction. The weight vector $\mathbf{w}_{LCMV}$ is composed of two weight vector components contributed by the signal subspace and noise subspace, respectively. In contrast, the ESB beamformer finds its optimal weight vector $\mathbf{w}_{ESB}$ from $\mathbf{w}_{LCMV}$ by discarding the weight vector component contributed by the noise subspace. For these two steered beam beamformers, the only *priori* knowledge for finding the optimal weight is the actual direction vector of the desired signal. However, some uncertainties in the spatial information result in a mismatch between the steering vector and the direction vector of the desired signal. Many results have been reported on how to improve the performance of the steered beam beamformers against the mismatch [3–8].

A spatial uncertainty which is seldom taken into account during the adaptation process is the actual electromagnetic characteristics of an antenna array system. In practice, array sensors have physical dimensions and certain radiation characteristics. Under the situation where the distance between two array sensors is too short to assume that the sensors are isotropic point sensors isolated from each other, each array sensor sees a different environment and, hence, produces different individual radiation pattern. This is because some of energy in an array sensor is coupled to the others. This phenomenon is referred to as mutual coupling (MC). All signals received by an antenna array are affected by MC and the data will be no longer independent. The MC between the array sensors can significantly change an antenna array's behavior and its communication characteristics [9–12]. The predicted array system performances may not be accurate when we ignore the MC effects. Recently, research endeavor has been devoted to tackle the MC effect for improving the performance of an antenna array beamformer [8, 10, 12, 13] and the performance of bearing estimation using a two-dimensional uniform circular array (2-D UCA) [26].

In this paper, we analyze the system performance in terms of the array output signal-to-interference-plus-noise ratio (SINR) for adaptive arrays of arbitrary geometry under the MC effects. The MC effects are taken into account by using a distortion matrix model which is widely considered in many recent reports [8–14]. This model describes how the individual array sensors are coupled with one another. According

to this model, we insert a mutual coupling matrix (MCM) in the data model for the signal received by an array beamformer. Each entry of the MCM represents the MC coefficient between two related array sensors and can be estimated from collected measurement data [11, 12, 14, 15]. We first investigate the performance of the LCMV beamformers which are widely applied for achieving beamforming with various goals [16–21]. The ESB beamformers find their optimal weight vector from that of the LCMV beamformers by discarding the weight vector component contributed by the noise subspace. Moreover, it was shown that the ESB beamformer has better convergence properties and is less sensitive to pointing errors than the LCMV beamformers [22–24]. The performance of the ESB beamformers in the presence of MC effects is also investigated. Theoretical formulas for expressing the output SINRs of the LCMV and ESB beamformers are derived, respectively. Compared to the result presented in [25], our SINR formulas provide insights into the influence of the MC effects on the performances of the LCMV beamformer and the ESB beamformer. From our theoretical results, we note that the ESB beamformer outperforms the LCMV beamformer because the LCMV beamformer has a lower output signal-to-noise power ratio (SNR) than the ESB beamformer. As to the output interference power, LCMV and ESB beamformers have about the same ability in suppressing the interference. The closed-form expression for the SINR is shown to accurately predict the SINR obtained in simulations. Moreover, the formulas for computing the eigenvalues of the signal correlation matrix are derived under MC effects. Simulation results show that the effect of MC degrades the LCMV beamformer's performance even for large intersensor spacings and reduces the eigenvalues associated with the signal sources for small intersensor spacings.

This paper is organized as follows. In Section 2, the LCMV and ESB beamformers are briefly reviewed. The effect of MC on the output SINR for each of LCMV beamformer and ESB beamformer is evaluated in Section 3. Section 4 presents computer simulation results. Finally, we conclude the paper in Section 5.

2. BACKGROUND

Let an antenna array of arbitrary geometry have M array sensors. A narrow-band far-field desired signal and J uncorrelated interferers are impinging on the array. The data vector received by the array can be expressed as follows:

$$\mathbf{x}(t) = \mathbf{A}\mathbf{s}(t) + \mathbf{n}(t), \tag{1}$$

where $\mathbf{s}(t) = [s_d(t)\ s_1(t) \ldots s_J(t)]^T$ contains the complex waveforms $s_d(t)$ of the desired signal and $s_j(t)$ of the jth interferer, $j = 1, 2, \ldots, J$, respectively, $\mathbf{A} = [\mathbf{a}_d\ \mathbf{a}_1\ \ldots\ \mathbf{a}_J]$ contains the direction vectors $\mathbf{a}_d$ of the desired signal and $\mathbf{a}_j$ of the jth interferer, $j = 1, 2, \ldots, J$, respectively, and $\mathbf{n}(t) = [n_1(t)\ n_2(t)\ \ldots\ n_M(t)]^T$ represents the spatially white background noise vector. The superscript T denotes transpose operation. Assume that $\mathbf{s}(t)$ and $\mathbf{n}(t)$ are uncorrelated, the $M \times M$ ensemble correlation matrix of $\mathbf{x}(t)$ is given by

$$\mathbf{R}_x = E\left\{\mathbf{x}(t)\mathbf{x}(t)^H\right\} = \mathbf{A}\mathbf{R}_s\mathbf{A}^H + \sigma_n^2\mathbf{I}_M, \tag{2}$$

where the superscript H denotes complex conjugate transpose, $\mathbf{R}_s = E\{\mathbf{s}(t)\mathbf{s}(t)^H\}$ denotes the signal correlation matrix, σ_n^2 is the noise power, and $\mathbf{I}_M$ is the identity matrix with size $M \times M$. Let the array use a weight vector $\mathbf{w} = [w_1\ w_2\ \ldots\ w_M]^T$ for processing the received data vector $\mathbf{x}(t)$ to produce the output signal $y(t) = \mathbf{w}^H\mathbf{x}(t)$. According to the LCMV beamforming [1], the optimal weight vector can be found by solving the following constrained optimization problem:

$$\text{Minimize } E\left\{|y(t)|^2\right\} = \mathbf{w}^H\mathbf{R}_x\mathbf{w} \quad \text{Subject to} \quad \mathbf{w}^H\mathbf{a}_s = 1, \tag{3}$$

where $\mathbf{a}_s$ is the steering vector in the look direction. Thus, the optimal weight vector is given by

$$\mathbf{w}_{LCMV} = \mu\mathbf{R}_x^{-1}\mathbf{a}_s, \tag{4}$$

where μ is given by $(\mathbf{a}_s^H\mathbf{R}_x^{-1}\mathbf{a}_s)^{-1}$. Assume that the received signal number is less than the array element number, i.e., $(J+1) < M$, the correlation matrix $\mathbf{R}_x$ can be eigendecomposed as

$$\mathbf{R}_x = \sum_{i=1}^{M} \lambda_i\mathbf{e}_i\mathbf{e}_i^H = \mathbf{E}_S\mathbf{\Lambda}_S\mathbf{E}_S^H + \mathbf{E}_N\mathbf{\Lambda}_N\mathbf{E}_N^H, \tag{5}$$

where the eigenvalues $\lambda_1 \geqq \lambda_2\ \geqq \ldots \geqq \lambda_{J+1} > \lambda_{J+2} = \ldots = \lambda_M = \sigma_n^2$ are the eigenvalues of $\mathbf{R}_x$ in descending order, $\mathbf{e}_i$ is the eigenvector associated with λ_i, $i = 1, 2, \ldots, M$, $\mathbf{E}_S = [\mathbf{e}_1\ \mathbf{e}_2\ \ldots\ \mathbf{e}_{J+1}]$ is the basis matrix spanning the signal-plus-interference subspace (SS), $\mathbf{\Lambda}_S = \text{diag}\{\lambda_1\ \lambda_2 \ldots \lambda_{J+1}\}$, $\mathbf{E}_N = [\mathbf{e}_{J+2} \ldots \mathbf{e}_M]$ is the basis matrix spanning the noise subspace (NS), and $\mathbf{\Lambda}_N = \sigma_n^2\mathbf{I}_{M-J-1}$. It is easy to show that the inverse of $\mathbf{R}_x$ is given as follows:

$$\mathbf{R}_x^{-1} = \sum_{i=1}^{M} \lambda_i^{-1}\mathbf{e}_i\mathbf{e}_i^H = \mathbf{E}_S\mathbf{\Lambda}_S^{-1}\mathbf{E}_S^H + \mathbf{E}_N\mathbf{\Lambda}_N^{-1}\mathbf{E}_N^H. \tag{6}$$

Accordingly, (4) can be rewritten as

$$\mathbf{w}_{LCMV} = \mu\mathbf{R}_x^{-1}\mathbf{a}_s = \mu\left[\mathbf{E}_S\mathbf{\Lambda}_S^{-1}\mathbf{E}_S^H + \mathbf{E}_N\mathbf{\Lambda}_N^{-1}\mathbf{E}_N^H\right]\mathbf{a}_s. \tag{7}$$

We note from (7) that the LCMV weight vector $\mathbf{w}_{LCMV}$ is contributed by the SS component $\mathbf{w}_{LCMVS}$ and the NS component $\mathbf{w}_{LCMVN}$, respectively. They are given by

$$\mathbf{w}_{LCMVS} = \mu \left[\mathbf{E}_S \mathbf{\Lambda}_S^{-1} \mathbf{E}_S^H\right] \mathbf{a}_s \tag{8}$$

$$\mathbf{w}_{LCMVN} = \mu \left[\mathbf{E}_N \mathbf{\Lambda}_N^{-1} \mathbf{E}_N^H\right] \mathbf{a}_s. \tag{9}$$

In contrast, the ESB beamformers discard $\mathbf{w}_{LCMVN}$ directly and takes only $\mathbf{w}_{LCMVS}$ as the optimal weight vector $\mathbf{w}_{ESB}$ given by [2]

$$\mathbf{w}_{ESB} = \mu_e [\mathbf{E}_S \mathbf{\Lambda}_S^{-1} \mathbf{E}_S^H] \mathbf{a}_s, \tag{10}$$

where μ_e is given by $(\mathbf{a}_s^H \mathbf{E}_S \mathbf{\Lambda}_S^{-1} \mathbf{E}_S^H \mathbf{a}_s)^{-1}$. When the steering vector $\mathbf{a}_s$ is set to the direction vector $\mathbf{a}_d$ of the desired signal, the NS component $\mathbf{w}_{LCMVN}$ is a zero vector according to the orthogonality between the direction vector of the desired signal and the noise subspace, i.e., $\mathbf{E}_N^H \mathbf{a}_s = \mathbf{E}_N^H \mathbf{a}_d = 0$. In this ideal case, the optimal weight vector obtained from $\mathbf{R}_x$ lies within the SS subspace. Consequently, both the LCMV beamformer and the ESB beamformer demonstrate the same system performance because $\mathbf{w}_{LCMV} = \mathbf{w}_{LCMVS} = \mathbf{w}_{ESB}$. However, due to some imperfections in practical environment, the computed $\mathbf{w}_{LCMV}$ does not remain in the signal subspace because $\mathbf{w}_{LCMVN}$ is not equal to zero. This leads to the performance degradation of the LCMV beamformers [2].

3. PERFORMANCE ANALYSES OF ARRAY BEAMFORMERS WITH MC EFFECTS

In this section, we evaluate the effect of MC on the performance in terms of output SINR for the LCMV and ESB beamformers, respectively. The effect of MC is taken into account by using a distortion matrix model [8–14]. According to this model, we insert a mutual coupling matrix (MCM) $\mathbf{C}$ in the data model for the received signal as follows:

$$\mathbf{x}_c(t) = \mathbf{CAs}(t) + \mathbf{n}(t). \tag{11}$$

In the following analysis, we consider the case of one interferer uncorrelated with the desired signal to simplify the presentation. Let the powers of the desired signal $s_d(t)$ and the interferer $s_1(t)$ be p_d and p_1, respectively. The data vector of (1) becomes

$$\mathbf{x}_c(t) = s_d(t)\mathbf{C}\mathbf{a}_d + s_1(t)\mathbf{C}\mathbf{a}_1 + \mathbf{n}(t), \tag{12}$$

where the subscript c denotes the case with MC effect. The $M \times M$ ensemble correlation matrix of $\mathbf{x}_c(t)$ is given by

$$\begin{aligned}\mathbf{R}_{xc} &= E\left\{\mathbf{x}_c(t)\mathbf{x}_c(t)^H\right\} = \mathbf{CAR}_s\mathbf{A}^H\mathbf{C}^H + \sigma_n^2\mathbf{I}_M = p_d\mathbf{C}\mathbf{a}_d\mathbf{a}_d^H\mathbf{C}^H \\ &\quad + p_1\mathbf{C}\mathbf{a}_1\mathbf{a}_1^H\mathbf{C}^H + \sigma_n^2\mathbf{I}_M,\end{aligned} \tag{13}$$

where $p_d = E\{s_d(t)s_d(t)^H\}$ and $p_1 = E\{s_1(t)s_1(t)^H\}$. Similar to (5), we have the eigendecomposition for $\mathbf{R}_{xc}$ as follows:

$$\mathbf{R}_{xc} = \sum_{i=1}^{M} \lambda_{ic}\mathbf{e}_{ic}\mathbf{e}_{ic}^H = \mathbf{E}_{Sc}\mathbf{\Lambda}_{Sc}\mathbf{E}_{Sc}^H + \mathbf{E}_{Nc}\mathbf{\Lambda}_{Nc}\mathbf{E}_{Nc}^H, \tag{14}$$

Let the unitary matrices $\mathbf{E} = [\mathbf{E}_S\mathbf{E}_N]$ based on (5) and $\mathbf{E}_C = [\mathbf{E}_{Sc}\mathbf{E}_{Nc}]$ based on (14), respectively. We obtain the following diagonal matrices from (5) and (14)

$$\mathbf{\Lambda}_{xx} = \mathbf{E}^H[\mathbf{R}_x]\mathbf{E} = \mathbf{E}^H\left[\mathbf{A}\mathbf{R}_s\mathbf{A}^H\right]\mathbf{E} + \mathbf{E}^H\left[\sigma_n^2\mathbf{I}_M\right]\mathbf{E} = \mathbf{\Lambda}_1 + \mathbf{\Lambda}_2, \tag{15}$$

$$\begin{aligned}\mathbf{\Lambda}_{xxc} &= \mathbf{E}_C^H[\mathbf{R}_{xc}]\mathbf{E}_C = \mathbf{E}_C^H\left[\mathbf{C}\mathbf{A}\mathbf{R}_s\mathbf{A}^H\mathbf{C}^H\right]\mathbf{E}_C + \mathbf{E}_C^H\left[\sigma_n^2\mathbf{I}_M\right]\mathbf{E}_C \\ &= \mathbf{\Lambda}_{1c} + \mathbf{\Lambda}_{2c},\end{aligned} \tag{16}$$

where

$$\begin{aligned}\mathbf{\Lambda}_1 &= \mathbf{E}^H\left[\mathbf{A}\mathbf{R}_s\mathbf{A}^H\right]\mathbf{E} = \mathrm{diag}\{\rho_1\ \rho_2\ 0\ \ldots\ 0\}, \\ \mathbf{\Lambda}_{1c} &= \mathbf{E}_C^H\left[\mathbf{C}\mathbf{A}\mathbf{R}_s\mathbf{A}^H\mathbf{C}^H\right]\mathbf{E}_C = \mathrm{diag}\{\rho_{1c}\ \rho_{2c}\ 0\ \ldots\ 0\}, \\ \mathbf{\Lambda}_2 &= \mathbf{E}^H\left[\sigma_n^2\mathbf{I}_M\right]\mathbf{E}, \qquad \mathbf{\Lambda}_{2c} = \mathbf{E}_C^H\left[\sigma_n^2\mathbf{I}_M\right]\mathbf{E}_C.\end{aligned} \tag{17}$$

The equality $\mathbf{\Lambda}_1 = \mathbf{E}^H[\mathbf{A}\mathbf{R}_s\mathbf{A}^H]\mathbf{E}$ leads to

$$\mathbf{A}\mathbf{R}_s\mathbf{A}^H = \mathbf{E}\mathbf{\Lambda}_1\mathbf{E}^H. \tag{18}$$

Substituting (18) into $\mathbf{\Lambda}_{1c} = \mathbf{E}_C^H[\mathbf{C}\mathbf{A}\mathbf{R}_s\mathbf{A}^H\mathbf{C}^H]\mathbf{E}_C$ yields $\mathbf{\Lambda}_{1c} = \mathbf{E}_C^H[\mathbf{C}\mathbf{E}\mathbf{\Lambda}_1\mathbf{E}^H\mathbf{C}^H]\mathbf{E}_C$ and

$$\mathbf{C}\mathbf{E}\mathbf{\Lambda}_1\mathbf{E}^H\mathbf{C}^H = \mathbf{E}_C\mathbf{\Lambda}_{1c}\mathbf{E}_C^H. \tag{19}$$

Expanding (19) and performing some manipulations gives

$$\begin{aligned}&\rho_1\mathbf{C}\mathbf{e}_1\mathbf{e}_1^H\mathbf{C}^H + \rho_2\mathbf{C}\mathbf{e}_2\mathbf{e}_2^H\mathbf{C}^H = \rho_{1c}\mathbf{e}_{1c}\mathbf{e}_{1c}^H + \rho_{2c}\mathbf{e}_{2c}\mathbf{e}_{2c}^H \\ =\ & p_d\mathbf{C}\mathbf{a}_d\mathbf{a}_d^H\mathbf{C}^H + p_1\mathbf{C}\mathbf{a}_1\mathbf{a}_1^H\mathbf{C}^H.\end{aligned} \tag{20}$$

Since $\mathbf{E}_C = [\mathbf{E}_{Sc}\mathbf{E}_{Nc}]$ is a unitary matrix, we have

$$\mathbf{E}_{Sc}\mathbf{E}_{Sc}^H + \mathbf{E}_{Nc}\mathbf{E}_{Nc}^H = \mathbf{I}_M. \tag{21}$$

It follows from (21) that

$$\mathbf{e}_{1c}\mathbf{e}_{1c}^H + \mathbf{e}_{2c}\mathbf{e}_{2c}^H = \mathbf{I}_M - \mathbf{E}_{Nc}\mathbf{E}_{Nc}^H. \tag{22}$$

Using (20) and (22), we obtain the following expressions for the eigenvectors $\mathbf{e}_{1c}$ and $\mathbf{e}_{2c}$

$$\begin{aligned}\mathbf{e}_{1c}\mathbf{e}_{1c}^H &= \frac{\rho_1\mathbf{C}\mathbf{e}_1\mathbf{e}_1^H\mathbf{C}^H + \rho_2\mathbf{C}\mathbf{e}_2\mathbf{e}_2^H\mathbf{C}^H - \rho_{2c}\left(\mathbf{I}_M - \mathbf{E}_{Nc}\mathbf{E}_{Nc}^H\right)}{\rho_{1c} - \rho_{2c}}, \\ \mathbf{e}_{2c}\mathbf{e}_{2c}^H &= \frac{\rho_1\mathbf{C}\mathbf{e}_1\mathbf{e}_1^H\mathbf{C}^H + \rho_2\mathbf{C}\mathbf{e}_2\mathbf{e}_2^H\mathbf{C}^H - \rho_{1c}\left(\mathbf{I}_M - \mathbf{E}_{Nc}\mathbf{E}_{Nc}^H\right)}{\rho_{2c} - \rho_{1c}}.\end{aligned} \tag{23}$$

Moreover, we have from (17) that the eigenvalues ρ_{1c} and ρ_{2c} of $\mathbf{CAR}_s\mathbf{A}^H\mathbf{C}^H$ satisfy

$$\begin{aligned}
\rho_{1c}+\rho_{2c} &= trace\left(\mathbf{CAR}_s\mathbf{A}^H\mathbf{C}^H\right) = trace\left(\mathbf{R}_s\mathbf{A}^H\mathbf{C}^H\mathbf{CA}\right) \\
&= trace\left(\begin{bmatrix} p_d & 0 \\ 0 & p_1 \end{bmatrix}\begin{bmatrix} \mathbf{a}_d^H\mathbf{C}^H \\ \mathbf{a}_1^H\mathbf{C}^H \end{bmatrix}\begin{bmatrix} \mathbf{Ca}_d & \mathbf{Ca}_1 \end{bmatrix}\right) \\
&= p_d\mathbf{a}_d^H\mathbf{C}^H\mathbf{Ca}_d + p_1\mathbf{a}_1^H\mathbf{C}^H\mathbf{Ca}_1, \\
\rho_{1c}\rho_{2c} &= \det\left(\mathbf{R}_s\mathbf{A}^H\mathbf{C}^H\mathbf{CA}\right) = \det\left(\begin{bmatrix} p_d & 0 \\ 0 & p_1 \end{bmatrix}\right) \\
&\quad \det\left(\begin{bmatrix} \mathbf{a}_d^H\mathbf{C}^H\mathbf{Ca}_d & \mathbf{a}_d^H\mathbf{C}^H\mathbf{Ca}_1 \\ \mathbf{a}_1^H\mathbf{C}^H\mathbf{Ca}_d & \mathbf{a}_1^H\mathbf{C}^H\mathbf{Ca}_1 \end{bmatrix}\right) \\
&= p_dp_1\left(\mathbf{a}_d^H\mathbf{C}^H\mathbf{Ca}_d\mathbf{a}_1^H\mathbf{C}^H\mathbf{Ca}_1 - \mathbf{a}_1^H\mathbf{C}^H\mathbf{Ca}_d\mathbf{a}_d^H\mathbf{C}^H\mathbf{Ca}_1\right).
\end{aligned} \tag{24}$$

From the formulas given by (24), we can easily compute ρ_{1c} and ρ_{2c} which are the nonzero eigenvalues of the signal correlation matrix in the presence of MC effects. Thus, the signal-related eigenvalues λ_{1c} and λ_{2c} of (14) are given by $\lambda_{1c}=\rho_{1c}+\sigma_n^2$ and $\lambda_{2c}=\rho_{2c}+\sigma_n^2$, respectively.

3.1. The Output SINR of the LCMV Beamformers

The optimal weight vector of the LCMV beamformers with $\mathbf{a}_s=\mathbf{a}_d$ is given by

$$\mathbf{w}_{LCMVc} = \mu_c\mathbf{R}_{xc}^{-1}\mathbf{a}_d, \tag{25}$$

where μ_c is given by $(\mathbf{a}_d^H\mathbf{R}_{xc}^{-1}\mathbf{a}_d)^{-1}$.

3.1.1. The Output Desired Signal Power

Using the optimal weight vector given by (25), we compute the desired signal power p_{do} at the array output

$$p_{do}=p_d\left|\mathbf{w}_{LCMVc}^H\mathbf{Ca}_d\right|^2=p_d\mu_c^2\left|\mathbf{a}_d^H\left[\mathbf{E}_{Sc}\mathbf{\Lambda}_{Sc}^{-1}\mathbf{E}_{Sc}^H+\mathbf{E}_{Nc}\mathbf{\Lambda}_{Nc}^{-1}\mathbf{E}_{Nc}^H\right]\mathbf{Ca}_d\right|^2. \tag{26}$$

From (26) and the derivation shown in Appendix A, p_{do} is given by

$$\begin{aligned}
p_{do} &= \frac{p_d\mu_c^2}{\left(\rho_{1c}+\sigma_n^2\right)^2\left(\rho_{2c}+\sigma_n^2\right)^2} \\
&\quad \left|\begin{array}{l} \left(p_d\mathbf{a}_d^H\mathbf{C}^H\mathbf{Ca}_d + p_1\mathbf{a}_1^H\mathbf{C}^H\mathbf{Ca}_1+\sigma_n^2\right)\mathbf{a}_d^H\mathbf{Ca}_d \\ -p_d\mathbf{a}_d^H\mathbf{Ca}_d\mathbf{a}_d^H\mathbf{C}^H\mathbf{Ca}_d - p_1\mathbf{a}_d^H\mathbf{Ca}_1\mathbf{a}_1^H\mathbf{C}^H\mathbf{Ca}_d \end{array}\right|^2.
\end{aligned} \tag{27}$$

3.1.2. The Output Interference Power

Using the optimal weight vector given by (25), we obtain the interference power p_{io} at the array output

$$p_{io} = p_1 \left| \mathbf{w}_{LCMVc}^H \mathbf{C}\mathbf{a}_1 \right|^2 = p_1 \mu_c^2 \left| \mathbf{a}_d^H \left[\mathbf{E}_{Sc} \mathbf{\Lambda}_{Sc}^{-1} \mathbf{E}_{Sc}^H + \mathbf{E}_{Nc} \mathbf{\Lambda}_{Nc}^{-1} \mathbf{E}_{Nc}^H \right] \mathbf{C}\mathbf{a}_1 \right|^2. \tag{28}$$

From (28) and the derivation shown in Appendix B, p_{io} is given by

$$\begin{aligned} p_{io} = & \\ & \frac{p_1 \mu_c^2}{(\rho_{1c} + \sigma_n^2)^2 (\rho_{2c} + \sigma_n^2)^2} \left| (p_d \mathbf{a}_d^H \mathbf{C}^H \mathbf{C}\mathbf{a}_d + p_1 \mathbf{a}_1^H \mathbf{C}^H \mathbf{C}\mathbf{a}_1 + \sigma_n^2) \mathbf{a}_d^H \mathbf{C}\mathbf{a}_1 \right. \\ & \left. - p_d \mathbf{a}_d^H \mathbf{C}\mathbf{a}_d \mathbf{a}_d^H \mathbf{C}^H \mathbf{C}\mathbf{a}_1 - p_1 \mathbf{a}_d^H \mathbf{C}\mathbf{a}_1 \mathbf{a}_1^H \mathbf{C}^H \mathbf{C}\mathbf{a}_1 \right|^2. \end{aligned} \tag{29}$$

3.1.3. The Output Noise Power

Using the optimal weight vector given by (25), we compute the noise power p_{no} at the array output

$$p_{no} = \sigma_n^2 |\mathbf{w}_{LCMVc}|^2 = \sigma_n^2 \mu_c^2 \mathbf{a}_d^H \left[\mathbf{E}_{Sc} \mathbf{\Lambda}_{Sc}^{-2} \mathbf{E}_{Sc}^H + \mathbf{E}_{Nc} \mathbf{\Lambda}_{Nc}^{-2} \mathbf{E}_{Nc}^H \right] \mathbf{a}_d. \tag{30}$$

From (30) and the derivation shown in Appendix C, p_{no} is given by

$$\begin{aligned} p_{no} = \sigma_n^2 \mu_c^2 & \frac{\left(\begin{array}{l} -\left(p_d \mathbf{a}_d^H \mathbf{C}^H \mathbf{C}\mathbf{a}_d + p_1 \mathbf{a}_1^H \mathbf{C}^H \mathbf{C}\mathbf{a}_1 + 2\sigma_n^2 \right) \\ \left(p_d \mathbf{a}_d^H \mathbf{C}\mathbf{a}_d \mathbf{a}_d^H \mathbf{C}^H \mathbf{a}_d + p_1 \mathbf{a}_d^H \mathbf{C}\mathbf{a}_1 \mathbf{a}_1^H \mathbf{C}^H \mathbf{a}_d \right) \\ + \left(p_d \mathbf{a}_d^H \mathbf{C}^H \mathbf{C}\mathbf{a}_d + p_1 \mathbf{a}_1^H \mathbf{C}^H \mathbf{C}\mathbf{a}_1 + \sigma_n^2 \right)^2 \\ \left(M - \mathbf{a}_d^H \mathbf{E}_{Nc} \mathbf{E}_{Nc}^H \mathbf{a}_d \right) + \rho_{1c} \rho_{2c} \left(\mathbf{a}_d^H \mathbf{E}_{Nc} \mathbf{E}_{Nc}^H \mathbf{a}_d - M \right) \end{array} \right)}{(\rho_{1c} + \sigma_n^2)^2 (\rho_{2c} + \sigma_n^2)^2} \\ & + \frac{1}{\sigma_n^2} \mu_c^2 \mathbf{a}_d^H \mathbf{E}_{Nc} \mathbf{E}_{Nc}^H \mathbf{a}_d. \end{aligned} \tag{31}$$

Following the results of (27), (29), and (31), it is easy to show that the output SINR of the LCMV beamformers is given by (D1) in Appendix D.

3.2. The Output SINR of the ESB Beamformers

The optimal weight vector of the ESB beamformers with $\mathbf{a}_s = \mathbf{a}_d$ is given by

$$\mathbf{w}_{ESBc} = \mu_{ce} \left[\mathbf{E}_{Sc} \mathbf{\Lambda}_{Sc}^{-1} \mathbf{E}_{Sc}^H \right] \mathbf{a}_d, \tag{32}$$

where μ_{ce} is given by $(\mathbf{a}_d^H \mathbf{E}_{Sc} \mathbf{\Lambda}_{Sc}^{-1} \mathbf{E}_{Sc}^H \mathbf{a}_d)^{-1}$ to satisfy the constraint $\mathbf{w}_{ESBc}^H \mathbf{a}_d = 1$.

3.2.1. The Output Desired Signal Power

Using the optimal weight vector given by (32), we compute the desired signal power p_{do} at the array output

$$p_{deo} = p_d \left|\mathbf{w}_{ESBc}^H \mathbf{C}\mathbf{a}_d\right|^2 = p_d \mu_{ce}^2 \left|\mathbf{a}_d^H [\mathbf{E}_{Sc}\mathbf{\Lambda}_{Sc}^{-1}\mathbf{E}_{Sc}^H]\mathbf{C}\mathbf{a}_d\right|^2. \quad (33)$$

From (33) and the fact that $\mathbf{a}_d^H[\mathbf{E}_{Nc}\mathbf{\Lambda}_{Nc}^{-1}\mathbf{E}_{Nc}^H]\mathbf{C}\mathbf{a}_d = 0$, we can use the similar manner shown by Appendix A to obtain p_{deo} as follows:

$$p_{deo} = \frac{p_d \mu_{ce}^2}{(\rho_{1c}+\sigma_n^2)^2(\rho_{2c}+\sigma_n^2)^2} \left|(p_d \mathbf{a}_d^H \mathbf{C}^H \mathbf{C}\mathbf{a}_d + p_1 \mathbf{a}_1^H \mathbf{C}^H \mathbf{C}\mathbf{a}_1 + \sigma_n^2)\mathbf{a}_d^H \mathbf{C}\mathbf{a}_d - p_d \mathbf{a}_d^H \mathbf{C}\mathbf{a}_d \mathbf{a}_d^H \mathbf{C}^H \mathbf{C}\mathbf{a}_d - p_1 \mathbf{a}_d^H \mathbf{C}\mathbf{a}_1 \mathbf{a}_1^H \mathbf{C}^H \mathbf{C}\mathbf{a}_d\right|^2. \quad (34)$$

3.2.2. The Output Interference Power

Using the optimal weight vector given by (32), we obtain the interference power p_{1o} at the array output

$$p_{ieo} = p_1 \left|\mathbf{w}_{ESBc}^H \mathbf{C}\mathbf{a}_1\right|^2 = p_1 \mu_{ce}^2 \left|\mathbf{a}_d^H \left[\mathbf{E}_{Sc}\mathbf{\Lambda}_{Sc}^{-1}\mathbf{E}_{Sc}^H\right] \mathbf{C}\mathbf{a}_1\right|^2. \quad (35)$$

From (35) and the fact that $\mathbf{a}_d^H[\mathbf{E}_{Nc}\mathbf{\Lambda}_{Nc}^{-1}\mathbf{E}_{Nc}^H]\mathbf{C}\mathbf{a}_1 = 0$, we can use the similar manner shown by Appendix B to obtain p_{ieo} as follows:

$$p_{ieo} = \frac{p_1 \mu_{ce}^2}{(\rho_{1c}+\sigma_n^2)^2 (\rho_{2c}+\sigma_n^2)^2} \left|(p_d \mathbf{a}_d^H \mathbf{C}^H \mathbf{C}\mathbf{a}_d + p_1 \mathbf{a}_1^H \mathbf{C}^H \mathbf{C}\mathbf{a}_1 + \sigma_n^2)\mathbf{a}_d^H \mathbf{C}\mathbf{a}_1 - p_d \mathbf{a}_d^H \mathbf{C}\mathbf{a}_d \mathbf{a}_d^H \mathbf{C}^H \mathbf{C}\mathbf{a}_1 - p_1 \mathbf{a}_d^H \mathbf{C}\mathbf{a}_1 \mathbf{a}_1^H \mathbf{C}^H \mathbf{C}\mathbf{a}_1\right|^2. \quad (36)$$

3.2.3. The Output Noise Power

Using the optimal weight vector given by (32), we compute the noise power p_{neo} at the array output

$$p_{neo} = \sigma_n^2 |\mathbf{w}_{ESBc}|^2 = \sigma_n^2 \mu_{ce}^2 \mathbf{a}_d^H \left[\mathbf{E}_{Sc}\mathbf{\Lambda}_{Sc}^{-2}\mathbf{E}_{Sc}^H\right] \mathbf{a}_d. \quad (37)$$

Following the same manner shown in Appendix C without considering the term $\sigma_n^2 \mu_{ce}^2 \mathbf{a}_d^H [\mathbf{E}_{Nc}\mathbf{\Lambda}_{Nc}^{-2}\boldsymbol{E}_{Nc}^H]\mathbf{a}_d$, we can easily obtain p_{neo} as follows:

$$p_{neo} = \sigma_n^2 \mu_{ce}^2 \frac{\begin{pmatrix} -\left(p_d \mathbf{a}_d^H \mathbf{C}^H \mathbf{C}\mathbf{a}_d + p_1 \mathbf{a}_1^H \mathbf{C}^H \mathbf{C}\mathbf{a}_1 + 2\sigma_n^2\right) \\ \left(p_d \mathbf{a}_d^H \mathbf{C}\mathbf{a}_d \mathbf{a}_d^H \mathbf{C}^H \mathbf{a}_d + p_1 \mathbf{a}_d^H \mathbf{C}\mathbf{a}_1 \mathbf{a}_1^H \mathbf{C}^H \mathbf{a}_d\right) \\ + \left(p_d \mathbf{a}_d^H \mathbf{C}^H \mathbf{C}\mathbf{a}_d + p_1 \mathbf{a}_1^H \mathbf{C}^H \mathbf{C}\mathbf{a}_1 + \sigma_n^2\right)^2 \\ \left(M - \mathbf{a}_d^H \mathbf{E}_{Nc}\mathbf{E}_{Nc}^H \mathbf{a}_d\right) + \rho_{1c}\rho_{2c}\left(\mathbf{a}_d^H \mathbf{E}_{Nc}\mathbf{E}_{Nc}^H \mathbf{a}_d - M\right) \end{pmatrix}}{(\rho_{1c}+\sigma_n^2)^2(\rho_{2c}+\sigma_n^2)^2}. \quad (38)$$

Following the results of (34), (36), and (38), it is easy to show that the output SINR of the ESB beamformers is given by (E1) of Appendix E.

Comparing (D1) and (E1), we observe that the denominator of SINR_{LCMV} has an additional term U given by:

$$\begin{aligned} U &= \frac{1}{\sigma_n^2}\left(p_d p_1\left(\mathbf{a}_d^H\mathbf{C}^H\mathbf{C}\mathbf{a}_d\mathbf{a}_1^H\mathbf{C}^H\mathbf{C}\mathbf{a}_1 - \mathbf{a}_1^H\mathbf{C}^H\mathbf{C}\mathbf{a}_d\mathbf{a}_d^H\mathbf{C}^H\mathbf{C}\mathbf{a}_1\right)\right. \\ &\quad \left. + \left(p_d\mathbf{a}_d^H\mathbf{C}^H\mathbf{C}\mathbf{a}_d + p_1\mathbf{a}_1^H\mathbf{C}^H\mathbf{C}\mathbf{a}_1\right)\sigma_n^2 + \sigma_n^4\right)^2\mathbf{a}_d^H\mathbf{E}_{Nc}\mathbf{E}_{Nc}^H\mathbf{a}_d \\ &= \frac{1}{\sigma_n^2}(\rho_{1c}\rho_{2c} + (\rho_{1c}+\rho_{2c})\sigma_n^2 + \sigma_n^4)^2\mathbf{a}_d^H\mathbf{E}_{Nc}\mathbf{E}_{Nc}^H\mathbf{a}_d \end{aligned} \tag{39}$$

according to (24). This term represents a positive quantity. Therefore, the ESB beamformers outperform the LCMV beamformers in the presence of MC effects since $\text{SINR}_{LCMV} < \text{SINR}_{ESB}$.

4. COMPUTER SIMULATION EXAMPLES

Here, we present several simulation examples for confirming the theoretical results. For all simulation examples, we adopt the MCM $\mathbf{C}$ suggested by [11, 12, 14, 15] as follows:

$$\mathbf{C} = (Z_A + Z_T)(\mathbf{Z} + Z_T\mathbf{I}_M\ )^{-1}, \tag{40}$$

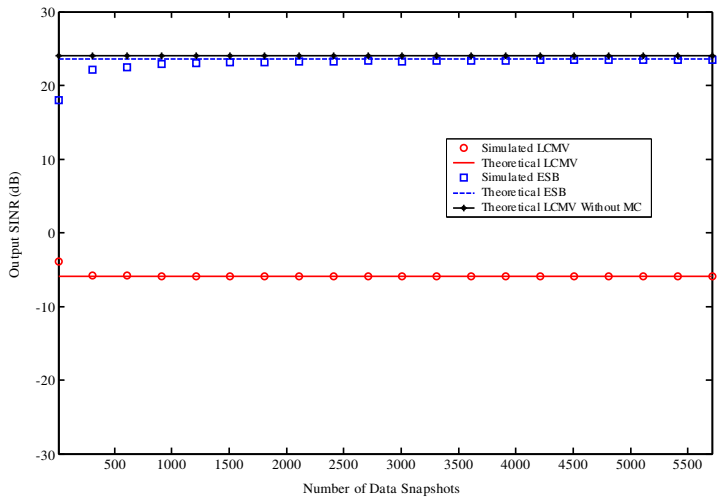

Figure 1. The output SINR versus number of snapshots for *Example 1.*

where Z_A is the sensor's impedance in isolation, Z_T is the impedance of the receiver at each sensor and is set to the complex conjugate of Z_A to achieve an impedance match for maximum power transfer. Consider the case of an antenna array with the side-by-side configuration and the dipole length $= \lambda/2$, where λ is the wavelength of signal sources. Then, $\mathbf{Z}$ is the mutual impedance matrix given by [11, 12, 14, 15]

$$\mathbf{Z} = \begin{bmatrix} Z_{11} & Z_{12} & \cdots & Z_{1M} \\ Z_{21} & Z_{22} & \cdots & Z_{2M} \\ \vdots & \vdots & \ddots & \vdots \\ Z_{M1} & Z_{M2} & \cdots & Z_{MM} \end{bmatrix}, \tag{41}$$

where the entry Z_{mn}, $1 \leqq m, n \leqq M$, is given by

$$Z_{mn} = \begin{cases} 30[0.5772 + \ln(2\kappa\gamma) - C_i(2\kappa\gamma)] + \mathrm{j}[30(S_i(2\kappa\gamma))] = \mathrm{Z}_A, \\ \qquad\qquad\qquad\qquad\qquad\qquad \text{for } m = n \\ 30[2C_i(\mu_0) - C_i(\mu_1) - C_i(\mu_2)] - \mathrm{j}[30(2S_i(\mu_0) \\ -S_i(\mu_1) - S_i(\mu_2))], \quad \text{for } m \neq n \end{cases}, \tag{42}$$

where $\kappa = 2\pi/\lambda$, $\gamma = \lambda/2$, $\mu_0 = \kappa d_h$, $\mu_1 = \kappa(\sqrt{d_h^2 + \gamma^2} + \gamma)$, $\mu_2 = \kappa(\sqrt{d_h^2 + \gamma^2} - \gamma)$, $\mathrm{j} = \sqrt{-1}$, d_h denotes the horizontal distance between the two array sensors, and $C_i(\alpha) = \int_{\infty}^{\alpha} (\cos(x)/x)dx$ and $S_i(\alpha) = \int_0^{\alpha} (\sin(x)/x)dx$ are the cosine and sine integrals, respectively. The plots of the magnitude of the normalized impedance matrix elements of $\mathbf{Z}$ for an array of $M = 12$ and $\gamma/\lambda = 0.5$ with terminating impedance $Z_T = Z_A$ for a linear and a circular array geometries, respectively can be found in the Figure 1 of [11]. The number M of array sensors is 8. All signals used for simulations are binary phase shift keying (BPSK) signals with rectangular pulse shape. The received noise is assumed to be complex additive white Gaussian noise with mean zero and variance equal to one. To avoid the finite sample effects, 30000 data snapshots are taken to compute the sample correlation matrices $\hat{\mathbf{R}}_{xc}$, $\hat{\mathbf{R}}_{dd}$, $\hat{\mathbf{R}}_{ii}$, and $\hat{\mathbf{R}}_{nn}$ for the received data vector, desired signal, interferer, and noise, respectively. The optimal weight vectors $\hat{\mathbf{w}}_{LCMVc}$ and $\hat{\mathbf{w}}_{ESBc}$ corresponding to the LCMV and ESB beamformers are obtained from (25) and (32) based on $\hat{\mathbf{R}}_{xc}$, respectively. Then, the simulated SINR_{LCMV} and SINR_{ESB} are calculated as follows:

$$\overline{\mathrm{SINR}}_{LCMV} = \frac{\hat{\mathbf{w}}_{LCMVc}^H \hat{\mathbf{R}}_{dd} \hat{\mathbf{w}}_{LCMVc}}{\hat{\mathbf{w}}_{LCMVc}^H \hat{\mathbf{R}}_{ii} \hat{\mathbf{w}}_{LCMVc} + \hat{\mathbf{w}}_{LCMVc}^H \hat{\mathbf{R}}_{nn} \hat{\mathbf{w}}_{LCMVc}}, \tag{43}$$

$$\overline{\mathrm{SINR}}_{ESB} = \frac{\hat{\mathbf{w}}_{ESBc}^H \hat{\mathbf{R}}_{dd} \hat{\mathbf{w}}_{ESBc}}{\hat{\mathbf{w}}_{ESBc}^H \hat{\mathbf{R}}_{ii} \hat{\mathbf{w}}_{ESBc} + \hat{\mathbf{w}}_{ESBc}^H \hat{\mathbf{R}}_{nn} \hat{\mathbf{w}}_{ESBc}}. \tag{44}$$

The number of Monte Carlo runs is 200. In contrast, the theoretical results obtained by using the theoretical formulas (D1) and (E1) are also presented for comparison in each example. To demonstrate the fact that $\text{SINR}_{LCMV} < \text{SINR}_{ESB}$ for each example, we present a figure plotting SINR_{ESB} (dB)-SINR_{LCMV} (dB) versus the power of the desired signal. From (D1) and (E1), it is easy to show that

$$\text{SINR}_{ESB}(\text{dB}) - \text{SINR}_{LCMV}(\text{dB}) = 10\log_{10}\left(1 + \frac{U}{V}\right), \qquad (45)$$

where V denotes the denominator of SINR_{ESB} and U is given by (39). The term $\mathbf{E}_{Nc}\mathbf{E}_{Nc}^H$ required by U and V of (45) is given by $\mathbf{I}_M - \mathbf{E}_{Sc}\mathbf{E}_{Sc}^H$, where $\mathbf{E}_{Sc}$ is obtained from the eigendecomposition of $\mathbf{R}_{xc}$ of (13).

Example 1: We consider that a desired signal with SNR equal to 15 dB and an interferer with SNR equal to 25 dB are impinging on a uniform linear array (ULA) from direction angles θ_s and θ_i equal to 40° and 60° off array broadside, respectively. The ratio of the spacing d between two adjacent sensors to the wavelength λ of the signals is set to 0.5. Figure 1 shows the output SINRs versus the number of data snapshots. Figure 2 plots the simulated difference $\overline{\text{SINR}}_{ESB} - \overline{\text{SINR}}_{LCMV}$ and the theoretical difference given by (45) versus the number of data snapshots. As we can see from Figures 1 and 2, the difference between the simulated and theoretical results is due to the finite sample effects when using a small number of data samples,

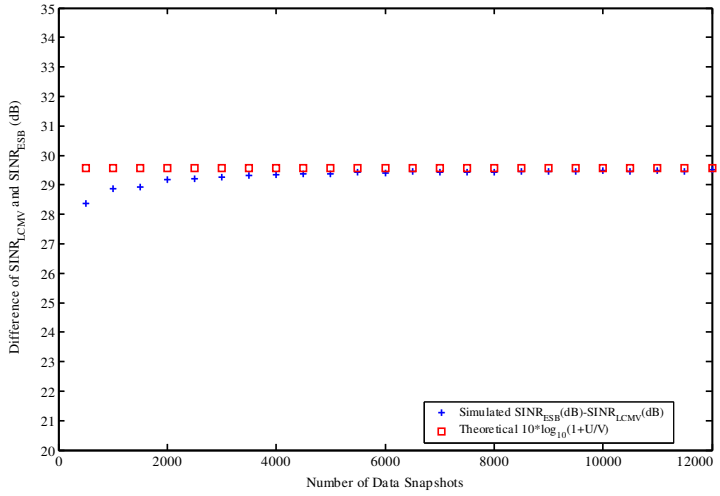

Figure 2. The output SINR difference versus number of snapshots for *Example 1*.

e.g., the number of data samples is less than 5000. Figure 3 depicts the output SINRs versus the desired signal power with the SNR of the interferer fixed at 25 dB. Figure 4 presents the simulated difference $\overline{\text{SINR}}_{ESB} - \overline{\text{SINR}}_{LCMV}$ and the theoretical difference given by (45) versus the desired signal power with the SNR of the interferer fixed at 25 dB, respectively. From these figures, we observe that the ESB beamformer outperforms the LCMV beamformer in the presence of MC effects. Moreover, the experimental results confirm the validity of the theoretical analyses presented in Section 3. We present array output SINR versus the intersensor spacing d in Figure 5. The MC affects the array performance of the LCMV beamformer significantly even for large intersensor spacing ($d > \lambda/2$). Figure 6 depicts the simulated difference $\overline{\text{SINR}}_{ESB} - \overline{\text{SINR}}_{LCMV}$ and the theoretical difference given by (45) versus the intersensor spacing d. Figure 7 shows the eigenvalues λ_{1c} and λ_{2c} versus the intersensor spacing d. We note that the MC reduces the eigenvalues associated with the signal sources for $d < \lambda$.

Example 2: We consider that a desired signal with signal-to-noise (SNR) equal to 15 dB and an interferer with SNR equal to 25 dB are impinging on a uniform circular array (UCA) from direction angles $[\phi_s, \theta_s]$ and $[\phi_i, \theta_i]$ equal to $[50°, 60°]$ and $[30°, 20°]$, respectively, where ϕ and θ represent the azimuth and elevation angles, respectively. The ratio of the spacing d between two adjacent sensors to the wavelength λ of the signals is set to 0.5. Figure 8 shows the output SINRs versus the number of data snapshots. Figure 9 plots the simulated difference

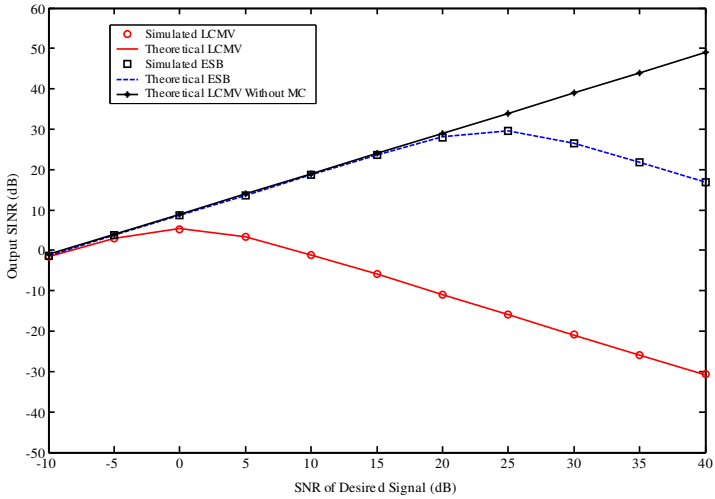

Figure 3. The output SINR versus desired signal power for *Example 1*.

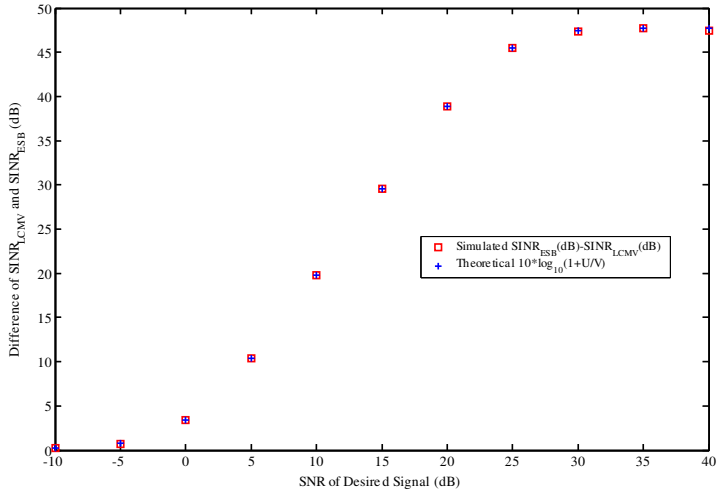

Figure 4. The output SINR difference versus desired signal power for *Example 1.*

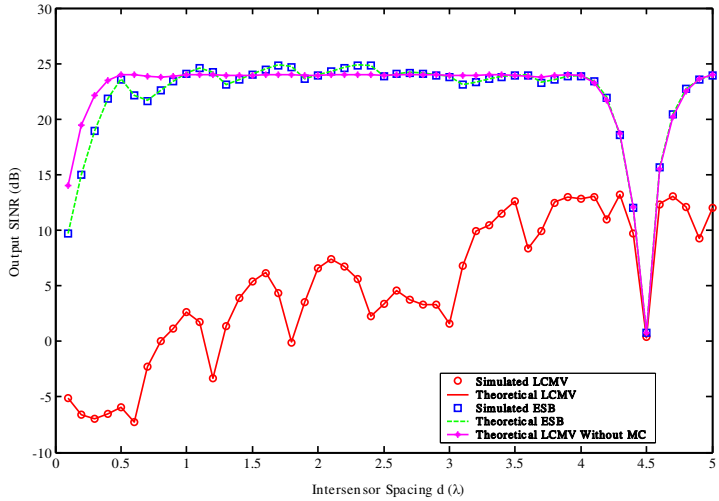

Figure 5. The output SINR versus inter-sensor spacing for *Example 1.*

$\overline{\text{SINR}}_{ESB} - \overline{\text{SINR}}_{LCMV}$ and the theoretical difference given by (45) versus the number of data snapshots. As we can see from Figures 8 and 9, the difference between the simulated and theoretical results is due to the finite sample effects when using a small number of data samples, e.g., the number of data samples is less than 5000. Figure 10

depicts the output SINRs versus the desired signal power with the SNR of the interferer fixed at 25 dB. Figure 11 presents the simulated difference $\overline{\text{SINR}}_{ESB} - \overline{\text{SINR}}_{LCMV}$ and the theoretical difference given

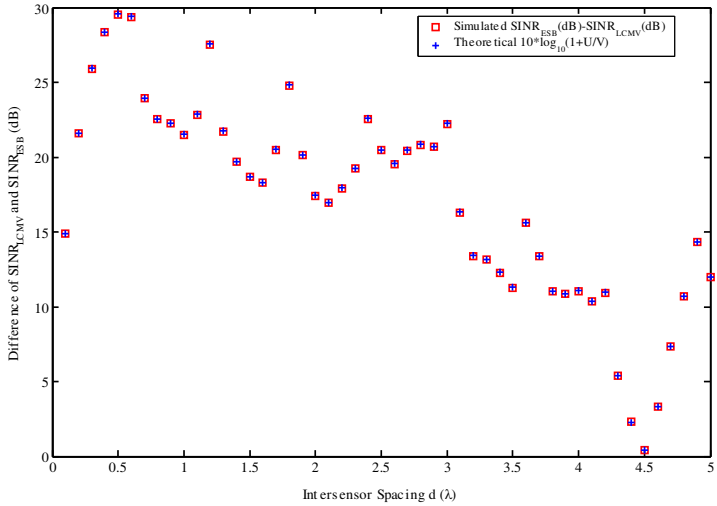

Figure 6. The output SINR difference versus inter-sensor spacing for *Example 1.*

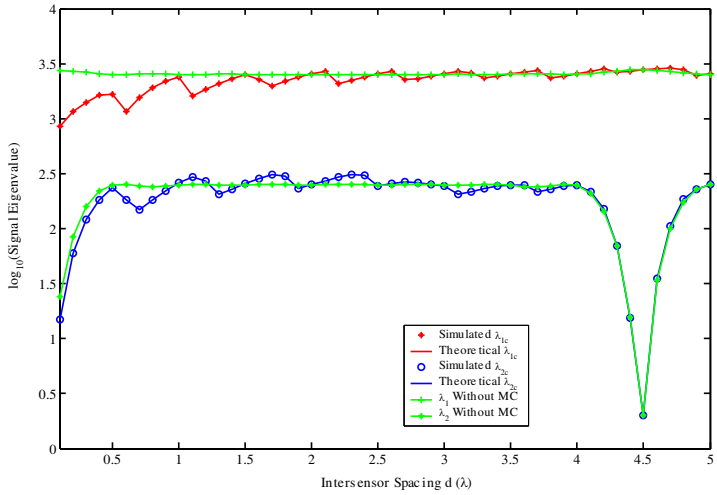

Figure 7. The signal eigenvalue versus inter-sensor spacing for *Example 1.*

by (45) versus the desired signal power with the SNR of the interferer fixed at 25 dB, respectively. From these figures, we observe that the ESB beamformer outperforms the LCMV beamformer in the presence of MC effects. Moreover, the experimental results confirm the validity

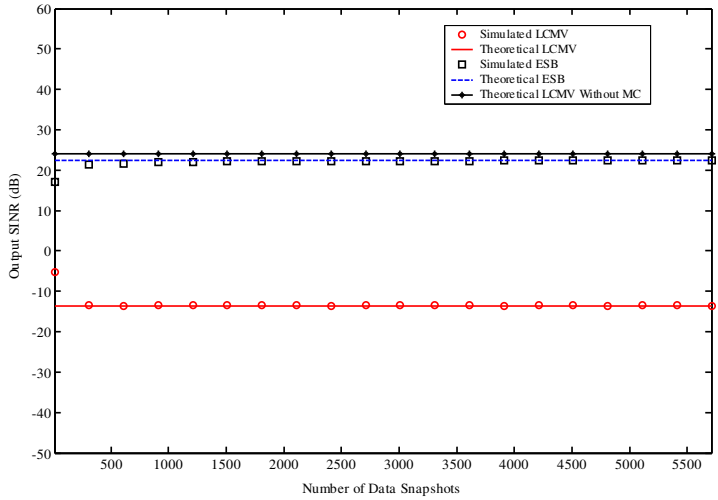

Figure 8. The output SINR versus number of snapshots for *Example 2*.

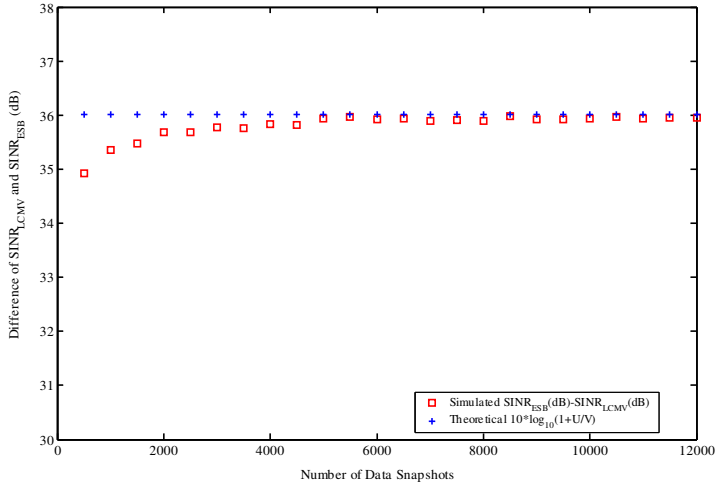

Figure 9. The output SINR difference versus number of snapshots for *Example 2*.

of the theoretical analyses presented in Section 3. We present array output SINR versus the intersensor spacing d in Figure 12. The MC affects the array performance of the LCMV beamformer significantly

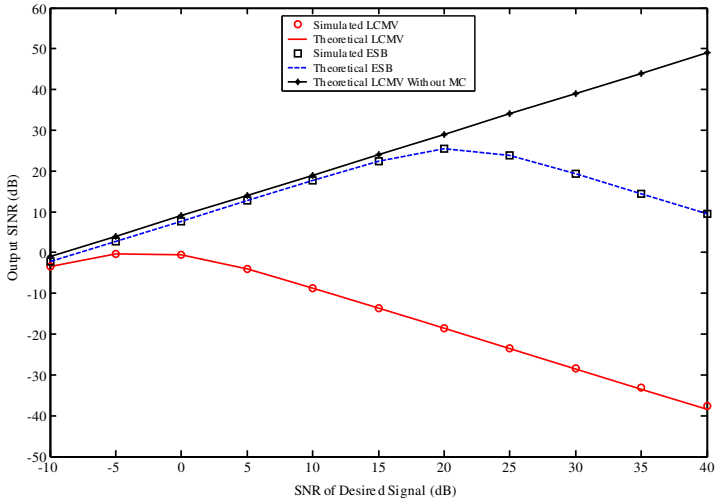

Figure 10. The output SINR versus the power of desired signal for *Example 2*.

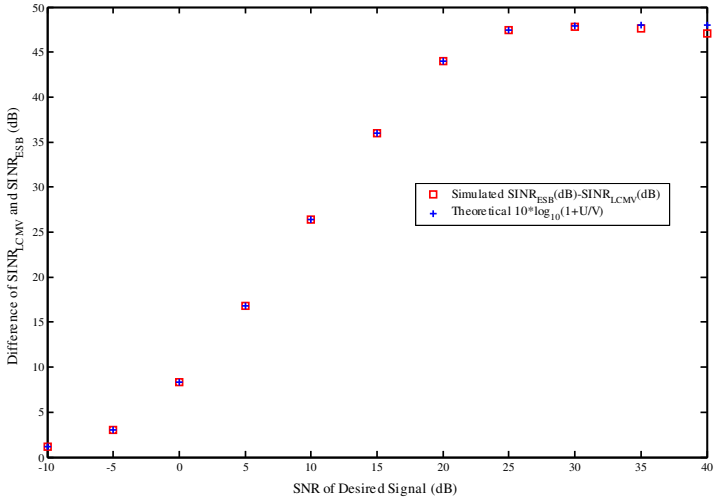

Figure 11. The output SINR difference versus the power of desired signal for *Example 2*.

even for large intersensor spacing ($d > \lambda/2$). Figure 13 depicts the simulated difference $\overline{\text{SINR}}_{ESB} - \overline{\text{SINR}}_{LCMV}$ and the theoretical difference given by (45) versus the intersensor spacing d. Figure 14

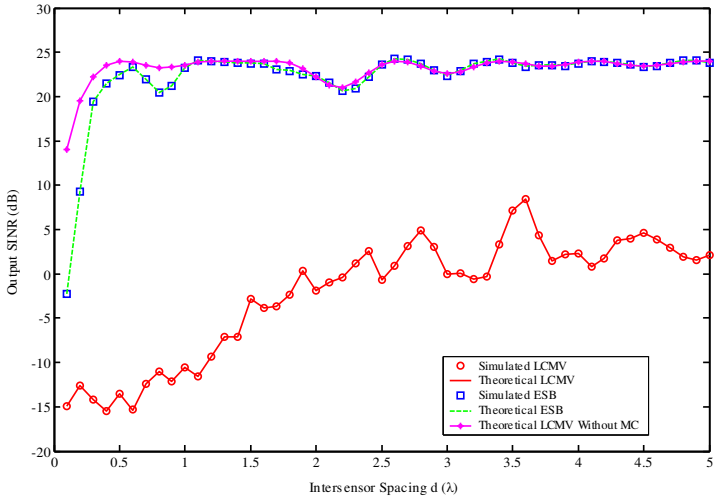

Figure 12. The output SINR versus inter-sensor spacing for *Example 2*.

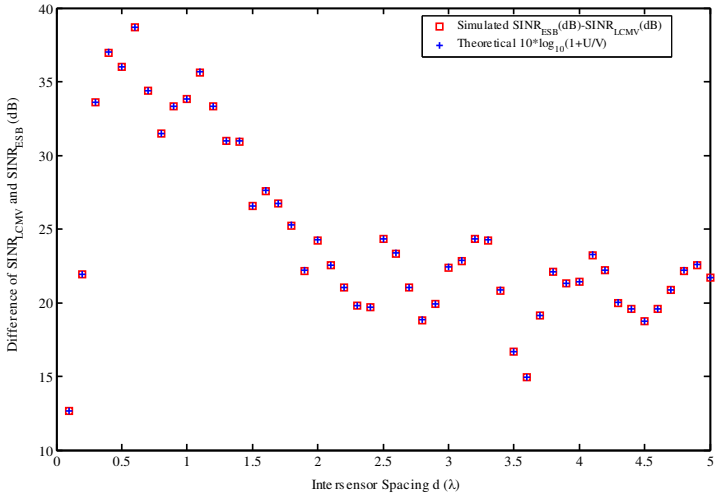

Figure 13. The SINR difference versus inter-sensor spacing for *Example 2*.

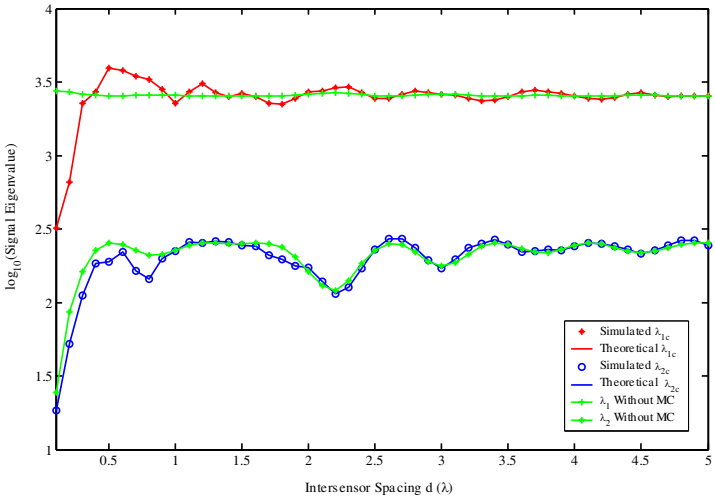

Figure 14. The signal eigenvalue versus inter-sensor spacing for *Example 2*.

shows the eigenvalues λ_{1c} and λ_{2c} versus the intersensor spacing d. We note that the MC reduces the eigenvalues associated with the signal sources for $d < 0.4\lambda$.

5. CONCLUSION

This paper has investigated the performance of adaptive array beamformers in the presence of the mutual coupling (MC) between array sensors. Using the model of a distortion matrix to encapsulate the MC effects, we have derived a closed-form expression for the output signal-to-interference-plus-noise ratio (SINR) for each of the linearly constrained minimum variance (LCMV) beamformer and the eigenspace-based (ESB) beamformer. The obtained SINR formulas provide insights into the influence of the MC effects on the performance of the array beamformers. It is shown that the ESB beamformer outperforms the LCMV beamformer under MC effects. The theoretical results are shown to accurately predict the SINRs obtained in simulations. Moreover, the effect of MC degrades the LCMV beamformer's performance even for large intersensor spacings and reduces the eigenvalues associated with the signal sources for small intersensor spacings. Finally, the derived theoretical SINR formulas can also be used to evaluate the influence of other spatial uncertainties on array beamformer's performance if the spatial uncertainties can be

represented by a distortion matrix model. Although it is not an easy task to derive the formulas for the case of multiple desired signals and interferers, we are currently investigating the possibility of obtaining the appropriate results based on the results presented in the paper.

APPENDIX A.

Derivation (27)

From (26), we have

$$p_{do} = p_d \mu_c^2 \left| \mathbf{a}_d^H \mathbf{E}_{Sc} \mathbf{\Lambda}_{Sc}^{-1} \mathbf{E}_{Sc}^H \mathbf{C} \mathbf{a}_d + \mathbf{a}_d^H \mathbf{E}_{Nc} \mathbf{\Lambda}_{Nc}^{-1} \mathbf{E}_{Nc}^H \mathbf{C} \mathbf{a}_d \right|^2 . \quad \text{(A1)}$$

Since the term $\mathbf{a}_d^H \mathbf{E}_{Nc} \mathbf{\Lambda}_{Nc}^{-1} \mathbf{E}_{Nc}^H \mathbf{C} \mathbf{a}_d = 0$, we only have to consider the term $\mathbf{a}_d^H \mathbf{E}_{Sc} \mathbf{\Lambda}_{Sc}^{-1} \mathbf{E}_{Sc}^H \mathbf{C} \mathbf{a}_d$. From (14), this term can be expanded as follows:

$$\begin{aligned} \mathbf{a}_d^H \mathbf{E}_{Sc} \mathbf{\Lambda}_{Sc}^{-1} \mathbf{E}_{Sc}^H \mathbf{C} \mathbf{a}_d &= \mathbf{a}_d^H \begin{bmatrix} \mathbf{e}_{1c} & \mathbf{e}_{2c} \end{bmatrix} \begin{bmatrix} \lambda_{1c} & 0 \\ 0 & \lambda_{2c} \end{bmatrix}^{-1} \begin{bmatrix} \mathbf{e}_{1c}^H \\ \mathbf{e}_{2c}^H \end{bmatrix} \mathbf{C} \mathbf{a}_d \\ &= \frac{1}{\lambda_{1c}} \mathbf{a}_d^H \mathbf{e}_{1c} \mathbf{e}_{1c}^H \mathbf{C} \mathbf{a}_d + \frac{1}{\lambda_{2c}} \mathbf{a}_d^H \mathbf{e}_{2c} \mathbf{e}_{2c}^H \mathbf{C} \mathbf{a}_d . \end{aligned} \quad \text{(A2)}$$

Substituting (23) into (A2) and performing some necessary manipulations yields

$$\begin{aligned} & \mathbf{a}_d^H \mathbf{E}_{Sc} \mathbf{\Lambda}_{Sc}^{-1} \mathbf{E}_{Sc}^H \mathbf{C} \mathbf{a}_d \\ = & \frac{\rho_1 \mathbf{a}_d^H \mathbf{C} \mathbf{e}_1 \mathbf{e}_1^H \mathbf{C}^H \mathbf{C} \mathbf{a}_d + \rho_2 \mathbf{a}_d^H \mathbf{C} \mathbf{e}_2 \mathbf{e}_2^H \mathbf{C}^H \mathbf{C} \mathbf{a}_d - \rho_{2c} \mathbf{a}_d^H \mathbf{C} \mathbf{a}_d}{(\rho_{1c} + \sigma_n^2)(\rho_{1c} - \rho_{2c})} \\ & - \frac{\rho_1 \mathbf{a}_d^H \mathbf{C} \mathbf{e}_1 \mathbf{e}_1^H \mathbf{C}^H \mathbf{C} \mathbf{a}_d + \rho_2 \mathbf{a}_d^H \mathbf{C} \mathbf{e}_2 \mathbf{e}_2^H \mathbf{C}^H \mathbf{C} \mathbf{a}_d - \rho_{1c} \mathbf{a}_d^H \mathbf{C} \mathbf{a}_d}{(\rho_{2c} + \sigma_n^2)(\rho_{1c} - \rho_{2c})} . \end{aligned} \quad \text{(A3)}$$

Substituting (20) and (A3) into (A1) and performing some necessary manipulations provides the output desired signal power shown by (27).

APPENDIX B.

Derivation (29)

From (28), we have

$$\begin{aligned} p_{io} &= p_1 \mu_c^2 \left| \mathbf{a}_d^H \left[\mathbf{E}_{Sc} \mathbf{\Lambda}_{Sc}^{-1} \mathbf{E}_{Sc}^H + \mathbf{E}_{Nc} \mathbf{\Lambda}_{Nc}^{-1} \mathbf{E}_{Nc}^H \right] \mathbf{C} \mathbf{a}_1 \right|^2 \\ &= p_1 \mu_c^2 |\mathbf{a}_d^H \mathbf{E}_{Sc} \mathbf{\Lambda}_{Sc}^{-1} \mathbf{E}_{Sc}^H \mathbf{C} \mathbf{a}_1|^2 . \end{aligned} \quad \text{(B1)}$$

Following (A2) and (A3), we can rewrite the term $\mathbf{a}_d^H \mathbf{E}_{Sc} \mathbf{\Lambda}_{Sc}^{-1} \mathbf{E}_{Sc}^H \mathbf{C}\mathbf{a}_1$ as

$$\begin{aligned}\mathbf{a}_d^H \mathbf{E}_{Sc} \mathbf{\Lambda}_{Sc}^{-1} \mathbf{E}_{Sc}^H \mathbf{C}\mathbf{a}_1 &= \frac{1}{\lambda_{1c}} \mathbf{a}_d^H \mathbf{e}_{1c} \mathbf{e}_{1c}^H \mathbf{C}\mathbf{a}_1 + \frac{1}{\lambda_{2c}} \mathbf{a}_d^H \mathbf{e}_{2c} \mathbf{e}_{2c}^H \mathbf{C}\mathbf{a}_1 \\ = & \frac{\rho_1 \mathbf{a}_d^H \mathbf{C}\mathbf{e}_1 \mathbf{e}_1^H \mathbf{C}^H \mathbf{C}\mathbf{a}_1 + \rho_2 \mathbf{a}_d^H \mathbf{C}\mathbf{e}_2 \mathbf{e}_2^H \mathbf{C}^H \mathbf{C}\mathbf{a}_1 - \rho_{2c} \mathbf{a}_d^H \mathbf{C}\mathbf{a}_1}{(\rho_{1c} + \sigma_n^2)(\rho_{1c} - \rho_{2c})} \\ & - \frac{\rho_1 \mathbf{a}_d^H \mathbf{C}\mathbf{e}_1 \mathbf{e}_1^H \mathbf{C}^H \mathbf{C}\mathbf{a}_1 + \rho_2 \mathbf{a}_d^H \mathbf{C}\mathbf{e}_2 \mathbf{e}_2^H \mathbf{C}^H \mathbf{C}\mathbf{a}_1 - \rho_{1c} \mathbf{a}_d^H \mathbf{C}\mathbf{a}_1}{(\rho_{2c} + \sigma_n^2)(\rho_{1c} - \rho_{2c})}. \quad \text{(B2)}\end{aligned}$$

Hence, substituting (20) and (B2) into (B1) and performing some necessary manipulations provides the output interference power shown by (29).

APPENDIX C.

Derivation (31)

Based on the data model given by (11), we note that the received noise is assumed to be spatially white and independent of the MC effects. It follows that

$$\mathbf{a}_d^H \mathbf{E}_{Nc} \mathbf{\Lambda}_{Nc}^{-2} \mathbf{E}_{Nc}^H \mathbf{a}_d = \mathbf{a}_d^H \mathbf{E}_{Nc} \mathbf{\Lambda}_N^{-2} \mathbf{E}_{Nc}^H \mathbf{a}_d = \frac{1}{\sigma_n^4} \mathbf{a}_d^H \mathbf{E}_{Nc} \mathbf{E}_{Nc}^H \mathbf{a}_d. \quad \text{(C1)}$$

From (30) and (C1), we have

$$\begin{aligned} p_{no} = & \sigma_n^2 \mu_c^2 \mathbf{a}_d^H \left[\mathbf{E}_{Sc} \mathbf{\Lambda}_{Sc}^{-2} \mathbf{E}_{Sc}^H + \mathbf{E}_{Nc} \mathbf{\Lambda}_{Nc}^{-2} \mathbf{E}_{Nc}^H \right] \mathbf{a}_d \\ = & \sigma_n^2 \mu_c^2 \left[\frac{1}{\lambda_{1c}^2} \mathbf{a}_d^H \mathbf{e}_{1c} \mathbf{e}_{1c}^H \mathbf{a}_d + \frac{1}{\lambda_{2c}^2} \mathbf{a}_d^H \mathbf{e}_{2c} \mathbf{e}_{2c}^H \mathbf{a}_d + \frac{1}{\sigma_n^4} \mathbf{a}_d^H \mathbf{E}_{Nc} \mathbf{E}_{Nc}^H \mathbf{a}_d \right]. \quad \text{(C2)} \end{aligned}$$

Substituting (23) into $\mathbf{a}_d^H \mathbf{E}_{Sc} \mathbf{\Lambda}_{Sc}^{-2} \mathbf{E}_{Sc}^H \mathbf{a}_d$ and performing some necessary manipulations yields

$$\begin{aligned} & \mathbf{a}_d^H \mathbf{E}_{Sc} \mathbf{\Lambda}_{Sc}^{-2} \mathbf{E}_{Sc}^H \mathbf{a}_d = \frac{1}{\lambda_{1c}^2} \mathbf{a}_d^H \mathbf{e}_{1c} \mathbf{e}_{1c}^H \mathbf{a}_d + \frac{1}{\lambda_{2c}^2} \mathbf{a}_d^H \mathbf{e}_{2c} \mathbf{e}_{2c}^H \mathbf{a}_d \\ = & \frac{\rho_1 \mathbf{a}_d^H \mathbf{C}\mathbf{e}_1 \mathbf{e}_1^H \mathbf{C}^H \mathbf{a}_d + \rho_2 \mathbf{a}_d^H \mathbf{C}\mathbf{e}_2 \mathbf{e}_2^H \mathbf{C}^H \mathbf{a}_d - \rho_{2c} \mathbf{a}_d^H \mathbf{a}_d + \rho_{2c} \mathbf{a}_d^H \mathbf{E}_{Nc} \mathbf{E}_{Nc}^H \mathbf{a}_d}{(\rho_{1c} + \sigma_n^2)^2 (\rho_{1c} - \rho_{2c})} \\ & - \frac{\rho_1 \mathbf{a}_d^H \mathbf{C}\mathbf{e}_1 \mathbf{e}_1^H \mathbf{C}^H \mathbf{a}_d + \rho_2 \mathbf{a}_d^H \mathbf{C}\mathbf{e}_2 \mathbf{e}_2^H \mathbf{C}^H \mathbf{a}_d - \rho_{1c} \mathbf{a}_d^H \mathbf{a}_d + \rho_{1c} \mathbf{a}_d^H \mathbf{E}_{Nc} \mathbf{E}_{Nc}^H \mathbf{a}_d}{(\rho_{2c} + \sigma_n^2)^2 (\rho_{1c} - \rho_{2c})} \\ = & \frac{\rho_1 \mathbf{a}_d^H \mathbf{C}\mathbf{e}_1 \mathbf{e}_1^H \mathbf{C}^H \mathbf{a}_d + \rho_2 \mathbf{a}_d^H \mathbf{C}\mathbf{e}_2 \mathbf{e}_2^H \mathbf{C}^H \mathbf{a}_d - M\rho_{2c} + \rho_{2c} \mathbf{a}_d^H \mathbf{E}_{Nc} \mathbf{E}_{Nc}^H \mathbf{a}_d}{(\rho_{1c} + \sigma_n^2)^2 (\rho_{1c} - \rho_{2c})} \\ & - \frac{\rho_1 \mathbf{a}_d^H \mathbf{C}\mathbf{e}_1 \mathbf{e}_1^H \mathbf{C}^H \mathbf{a}_d + \rho_2 \mathbf{a}_d^H \mathbf{C}\mathbf{e}_2 \mathbf{e}_2^H \mathbf{C}^H \mathbf{a}_d - M\rho_{1c} + \rho_{1c} \mathbf{a}_d^H \mathbf{E}_{Nc} \mathbf{E}_{Nc}^H \mathbf{a}_d}{(\rho_{2c} + \sigma_n^2)^2 (\rho_{1c} - \rho_{2c})} \quad \text{(C3)} \end{aligned}$$

since $\mathbf{a}_d^H \mathbf{a}_d = M$. Next, substituting (20) and (C3) into (C2) and performing some necessary manipulations provides the output interference power shown by (31).

APPENDIX D.

$$\mathrm{SINR}_{LCMV} = p_{do}/(p_{io} + p_{no}) =$$

$$\frac{\begin{pmatrix} p_d \left|(p_d \mathbf{a}_d^H \mathbf{C}^H \mathbf{C}\mathbf{a}_d + p_1 \mathbf{a}_1^H \mathbf{C}^H \mathbf{C}\mathbf{a}_1 + \sigma_n^2)\mathbf{a}_d^H \mathbf{C}\mathbf{a}_d \right. \\ \left. -p_d \mathbf{a}_d^H \mathbf{C}\mathbf{a}_d \mathbf{a}_d^H \mathbf{C}^H \mathbf{C}\mathbf{a}_d - p_1 \mathbf{a}_d^H \mathbf{C}\mathbf{a}_1 \mathbf{a}_1^H \mathbf{C}^H \mathbf{C}\mathbf{a}_d \right|^2 \end{pmatrix}}{\begin{pmatrix} p_1 \left|(p_d \mathbf{a}_d^H \mathbf{C}^H \mathbf{C}\mathbf{a}_d + p_1 \mathbf{a}_1^H \mathbf{C}^H \mathbf{C}\mathbf{a}_1 + \sigma_n^2)\mathbf{a}_d^H \mathbf{C}\mathbf{a}_1 \right. \\ \left. -p_d \mathbf{a}_d^H \mathbf{C}\mathbf{a}_d \mathbf{a}_d^H \mathbf{C}^H \mathbf{C}\mathbf{a}_1 - p_1 \mathbf{a}_d^H \mathbf{C}\mathbf{a}_1 \mathbf{a}_1^H \mathbf{C}^H \mathbf{C}\mathbf{a}_1 \right|^2 \\ +\sigma_n^2 \begin{pmatrix} -\left(p_d \mathbf{a}_d^H \mathbf{C}^H \mathbf{C}\mathbf{a}_d + p_1 \mathbf{a}_1^H \mathbf{C}^H \mathbf{C}\mathbf{a}_1 + 2\sigma_n^2\right) \\ \left(p_d \mathbf{a}_d^H \mathbf{C}\mathbf{a}_d \mathbf{a}_d^H \mathbf{C}^H \mathbf{a}_d + p_1 \mathbf{a}_d^H \mathbf{C}\mathbf{a}_1 \mathbf{a}_1^H \mathbf{C}^H \mathbf{a}_d\right) \\ +\left(p_d \mathbf{a}_d^H \mathbf{C}^H \mathbf{C}\mathbf{a}_d + p_1 \mathbf{a}_1^H \mathbf{C}^H \mathbf{C}\mathbf{a}_1 + \sigma_n^2\right)^2 \\ \left(M - \mathbf{a}_d^H \mathbf{E}_{Nc} \mathbf{E}_{Nc}^H \mathbf{a}_d\right) \\ -p_d p_1 \left(\mathbf{a}_d^H \mathbf{C}^H \mathbf{C}\mathbf{a}_d \mathbf{a}_1^H \mathbf{C}^H \mathbf{C}\mathbf{a}_1 - \mathbf{a}_1^H \mathbf{C}^H \mathbf{C}\mathbf{a}_d \mathbf{a}_d^H \mathbf{C}^H \mathbf{C}\mathbf{a}_1\right) \\ \left(M - \mathbf{a}_d^H \mathbf{E}_{Nc} \mathbf{E}_{Nc}^H \mathbf{a}_d\right) \end{pmatrix} \\ +\frac{1}{\sigma_n^2}(p_d p_1 (\mathbf{a}_d^H \mathbf{C}^H \mathbf{C}\mathbf{a}_d \mathbf{a}_1^H \mathbf{C}^H \mathbf{C}\mathbf{a}_1 - \mathbf{a}_1^H \mathbf{C}^H \mathbf{C}\mathbf{a}_d \mathbf{a}_d^H \mathbf{C}^H \mathbf{C}\mathbf{a}_1) \\ +(p_d \mathbf{a}_d^H \mathbf{C}^H \mathbf{C}\mathbf{a}_d + p_1 \mathbf{a}_1^H \mathbf{C}^H \mathbf{C}\mathbf{a}_1)\sigma_n^2 + \sigma_n^4)^2 \mathbf{a}_d^H \mathbf{E}_{Nc} \mathbf{E}_{Nc}^H \mathbf{a}_d \end{pmatrix}} \quad \text{(D1)}$$

APPENDIX E.

$$\mathrm{SINR}_{ESB} = p_{deo}/(p_{ieo} + p_{neo}) =$$

$$\frac{\begin{pmatrix} p_d \left|(p_d \mathbf{a}_d^H \mathbf{C}^H \mathbf{C}\mathbf{a}_d + p_1 \mathbf{a}_1^H \mathbf{C}^H \mathbf{C}\mathbf{a}_1 + \sigma_n^2)\mathbf{a}_d^H \mathbf{C}\mathbf{a}_d \right. \\ \left. -p_d \mathbf{a}_d^H \mathbf{C}\mathbf{a}_d \mathbf{a}_d^H \mathbf{C}^H \mathbf{C}\mathbf{a}_d - p_1 \mathbf{a}_d^H \mathbf{C}\mathbf{a}_1 \mathbf{a}_1^H \mathbf{C}^H \mathbf{C}\mathbf{a}_d \right|^2 \end{pmatrix}}{\begin{pmatrix} p_1 \left|(p_d \mathbf{a}_d^H \mathbf{C}^H \mathbf{C}\mathbf{a}_d + p_1 \mathbf{a}_1^H \mathbf{C}^H \mathbf{C}\mathbf{a}_1 + \sigma_n^2)\mathbf{a}_d^H \mathbf{C}\mathbf{a}_1 \right. \\ \left. -p_d \mathbf{a}_d^H \mathbf{C}\mathbf{a}_d \mathbf{a}_d^H \mathbf{C}^H \mathbf{C}\mathbf{a}_1 - p_1 \mathbf{a}_d^H \mathbf{C}\mathbf{a}_1 \mathbf{a}_1^H \mathbf{C}^H \mathbf{C}\mathbf{a}_1 \right|^2 \\ +\sigma_n^2 \begin{pmatrix} -\left(p_d \mathbf{a}_d^H \mathbf{C}^H \mathbf{C}\mathbf{a}_d + p_1 \mathbf{a}_1^H \mathbf{C}^H \mathbf{C}\mathbf{a}_1 + 2\sigma_n^2\right) \\ \left(p_d \mathbf{a}_d^H \mathbf{C}\mathbf{a}_d \mathbf{a}_d^H \mathbf{C}^H \mathbf{a}_d + p_1 \mathbf{a}_d^H \mathbf{C}\mathbf{a}_1 \mathbf{a}_1^H \mathbf{C}^H \mathbf{a}_d\right) \\ +(p_d \mathbf{a}_d^H \mathbf{C}^H \mathbf{C}\mathbf{a}_d + p_1 \mathbf{a}_1^H \mathbf{C}^H \mathbf{C}\mathbf{a}_1 + \sigma_n^2)^2 \\ (M - \mathbf{a}_d^H \mathbf{E}_{Nc} \mathbf{E}_{Nc}^H \mathbf{a}_d) \\ -p_d p_1 \left(\mathbf{a}_d^H \mathbf{C}^H \mathbf{C}\mathbf{a}_d \mathbf{a}_1^H \mathbf{C}^H \mathbf{C}\mathbf{a}_1 - \mathbf{a}_1^H \mathbf{C}^H \mathbf{C}\mathbf{a}_d \mathbf{a}_d^H \mathbf{C}^H \mathbf{C}\mathbf{a}_1\right) \\ (M - \mathbf{a}_d^H \mathbf{E}_{Nc} \mathbf{E}_{Nc}^H \mathbf{a}_d) \end{pmatrix} \end{pmatrix}}. \quad \text{(E1)}$$

ACKNOWLEDGMENT

This work was supported by the National Science Council of TAIWAN under Grants NSC96-2221-E002-086 and NSC97-2221-E002-174-MY3.

REFERENCES

1. Frost, O. L., III, "An algorithm for linearly constrained adaptive array processing," *Proc. IEEE*, Vol. 60, No. 8, 926–935, Aug. 1972.
2. Chang, L. and C.-C. Yeh, "Performance of DMI and eigenspace-based beamformers," *IEEE Trans. Antennas and Propagat.*, Vol. 40, No. 11, 1336–1347, Nov. 1992.
3. Cox, H., R. M. Zeskind, and M. M. Owen, "Robust adaptive beamforming," *IEEE Trans. Acoust., Speech, Signal Processing*, Vol. 35, No. 10, 1365–1375, Oct. 1987.
4. Zhang, S. and I. L. Thng, "Robust presteering derivative constraints for broadband antenna arrays," *IEEE Trans. Signal Processing*, Vol. 50, No. 1, 1–10, Jan. 2002.
5. Vorobyov, S. A., A. B. Gershman, and Z. Luo, "Robust adaptive beamforming using worst-case performance optimization: A solution to the signal mismatch problem," *IEEE Trans. Signal Processing*, Vol. 51, No. 2, 313–324, Feb. 2003.
6. Shahbazpanahi, S., A. B. Gershman, Z. Q. Luo, and K. M. Wong, "Robust adaptive beamforming for general-rank signal model," *IEEE Trans. Signal Processing,* Vol. 51, No. 9, 2257–2269, Sep. 2003.
7. Zou, Q., Z. L. Yu, and Z. Lin, "A robust algorithm for linearly constrained adaptive beamforming," *IEEE Signal Processing Letters*, Vol. 11, No. 1, 26–29, Jan. 2004.
8. Elnashar, A., S. M. Elnoubi, and H. A. El-Mikati, "Further study on robust adaptive beamforming with optimum diagonal loading," *IEEE Trans. Antennas Propagat.*, Vol. 54, No. 12, 3647–3658, Dec. 2006.
9. Svantesson, T. and A. Ranheim, "Mutual coupling effects on the capacity of multielement antenna systems," *Proc. of IEEE International Conference on Acoust., Speech, Signal Processing*, Vol. 4, 2485–2488, Salt City, UT, USA, May 2001.
10. Dandekar, K. R., H. Ling, and G. Xu, "Experimental study of mutual coupling compensation in smart antenna applications," *IEEE Trans. Wireless Communications*, Vol. 1, No. 3, 480–487, Jul. 2002.
11. Durrani, S. and M. E. Bialkowski, "Effect of mutual coupling on

the interference rejection capabilities of linear and circular arrays in CDMA systems," *IEEE Trans. Antennas Propagat.*, Vol. 52, No. 4, 1130–1134, Apr. 2004.

12. Huang, Z., C. A. Balanis, and C. R. Birtcher, "Mutual coupling compensation in UCAs: Simulations and experiment," *IEEE Trans. Antennas Propagat.*, Vol. 54, No. 11, 3082–3086, Nov. 2006.
13. Kikuchi, S., H. Tsuji, and A. Sano, "Autocalibration algorithm for robust Capon beamforming," *IEEE Trans. Antennas and Wireless Propagation Letters*, Vol. 5, 251–255, Dec. 2006.
14. Svantesson, T., "Modeling and estimation of mutual coupling in a uniform linear array of dipoles," *Proc. of IEEE International Conference on Acoust., Speech, Signal Processing*, Vol. 5, 2961–2964, Phoenix, AZ, USA, Mar. 1999.
15. Balanis, C. A., *Antenna Theory: Analysis and Design,* 3rd edition, John Wiley, New York, 2005.
16. Winters, J. H., "Smart antennas for wireless systems," *IEEE Pers. Commun. Mag.*, Vol. 5, No. 1, 23–27, Feb. 1998.
17. Trees, H. L. V., *Optimum Array Processing, Part IV of Detection, Estimation, and Modulation Theory*, Wiley Interscience, New York, 2002.
18. Hasna, M. O., M.-S. Alouini, A. Bastami, and E. S. Ebbini, "Performance analysis of cellular mobile systems with successive co-channel interference cancellation," *IEEE Trans. Wireless Commun.*, Vol. 2, No. 1, 29–40, Jan. 2003.
19. Kang, M., M.-S. Alouini, and L. Yang, "Outage probability and spectrum efficiency of cellular mobile radio systems with smart antennas," *IEEE Trans. Commun.*, Vol. 50, No. 12, 1871–1877, Dec. 2002.
20. Mostafa, R., A. Annamalai, and J. H. Reed, "Performance evaluation of cellular mobile radio systems with interference nulling of dominant interferers," *IEEE Trans. Commun.*, Vol. 52, No. 2, 326–335, Feb. 2004.
21. Li, H., Y.-D. Yao, and J. Yu, "Outage probabilities of wireless systems with LCMV beamforming," *IEEE Trans. Wireless Commun.*, Vol. 6, No. 10, 3515–3523, Oct. 2007.
22. Yu, S.-J. and J.-H. Lee, "Statistical performance of eigenspace-based adaptive array beamformers," *IEEE Trans. Antennas Propagat.*, Vol. 44, No. 5, 665–671, May 1996.
23. Lee, C.-C. and J.-H. Lee, "Eigenspace-based adaptive array beamforming with robust capabilities," *IEEE Trans. Antennas Propagat.*, Vol. 45, No. 12, 1711–1716, Dec. 1997.

24. Chang, L. and C. C. Yeh, "Effect of pointing errors on the performance of the projection beamformer," *IEEE Trans. Antennas Propagat.,* Vol. 41, No. 8, 1045–1056, Aug. 1993.
25. Gupta, I. J. and A. A. Ksienski, "Effect of mutual coupling on the performance of adaptive arrays," *IEEE Trans. Antennas Propagat.,* Vol. 31, No. 5, 785–791, Sep. 1983.
26. Xie, J., Z. S. He, and H.-Y. Li, "A fast DOA estimation algorithm for uniform circular arrays in the presence of unknown mutual coupling," *Progress In Electromagnetics Research C*, Vol. 21, 257–271, 2011.